SEQUENCES OF COMPATIBLE PERIODIC HYBRID ORBITS OF PREFRACTAL KOCH SNOWFLAKE BILLIARDS

MICHEL L. LAPIDUS AND ROBERT G. NIEMEYER

University of California, Riverside, 900 Big Springs Rd., Riverside, CA 92521, USA

(Communicated by Renato Feres)

ABSTRACT. The Koch snowflake KS is a nowhere differentiable curve. The billiard table $\Omega(KS)$ with boundary KS is, a priori, not well defined. That is, one cannot a priori determine the minimal path traversed by a billiard ball subject to a collision in the boundary of the table. It is this problem which makes $\Omega(KS)$ such an interesting, yet difficult, table to analyze.

In this paper, we approach this problem by approximating (from the inside) $\Omega(KS)$ by well-defined (prefractal) rational polygonal billiard tables $\Omega(KS_n)$. We first show that the flat surface $\mathcal{S}(KS_n)$ determined from the rational billiard $\Omega(KS_n)$ is a branched cover of the singly punctured hexagonal torus. Such a result, when combined with the results of [6], allows us to define a sequence of compatible orbits of prefractal billiards $\Omega(KS_n)$. Using a particular addressing system, we define a hybrid orbit of a prefractal billiard $\Omega(KS_n)$ and show that every dense orbit of a prefractal billiard $\Omega(KS_n)$ is a dense hybrid orbit of $\Omega(KS_n)$. This result is key in obtaining a topological dichotomy for a sequence of compatible orbits. Furthermore, we determine a sufficient condition for a sequence of compatible orbits to be a sequence of compatible *periodic hybrid* orbits.

We then examine the limiting behavior of a sequence of compatible periodic hybrid orbits. We show that the trivial limit of particular (eventually) constant sequences of compatible hybrid orbits constitutes an orbit of $\Omega(KS)$. In addition, we show that the union of two suitably chosen nontrivial polygonal paths connects two elusive limit points of the Koch snowflake. We conjecture that such a path is indeed the subset of what will eventually be an orbit of the Koch snowflake fractal billiard, once an appropriate 'fractal law of reflection' is determined.

Finally, we close with a discussion of several open problems and potential directions for further research. We discuss how it may be possible for our results to be generalized to other fractal billiard tables and how understanding the structures of the Veech groups of the prefractal billiards may help in determining '*fractal flat surfaces*' naturally associated with the billiard flows.
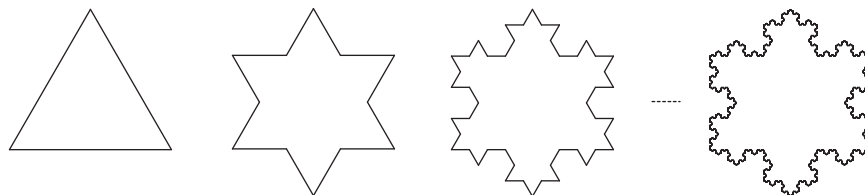
FIGURE 1. The Koch snowflake curve KS and its prefractal approximations KS_n, for $n = 0, 1, 2, \cdots$. As is well known, KS is a fractal, nowhere differentiable and closed curve, of infinite length and enclosing a finite area. Furthermore, it is self-similar; more precisely, it is the union of three abutting self-similar sets, each an isometric copy of the classic Koch curve. (See, e.g., [3].)

1. **Introduction.** The Koch snowflake curve KS, the construction of which is depicted in Figure 1, is everywhere nondifferentiable. The absence of a well-defined tangent at any point of KS is what, a priori, prevents one from determining a billiard flow on the billiard $\Omega(KS)$ with boundary KS. Indeed, since every point of KS is apparently a singularity of the billiard flow, one cannot a priori find a minimal path traversed by a billiard ball subject to a collision in the boundary. Our search for a solution to this problem will be, in part, motivated by the discussion on experimental results given in our earlier paper [12].

For each $n = 0, 1, 2, ...$, the prefractal KS_n is the nth (inner) polygonal approximation to KS, and defines a rational polygonal billiard table $\Omega(KS_n)$; that is, a polygon whose interior angles are all rational multiples of π. (See Figure 1.) Since the theory of rational polygonal billiards is very well developed (see, e.g., [4, 5, 7, 8, 9, 10, 11, 17, 18, 20, 21, 22, 23, 24, 26]), it is natural to want to define the dynamics on the fractal "billiard table" $\Omega(KS)$ in terms of the dynamics on its prefractal approximations $\Omega(KS_n)$. The focus of this paper is then to build a foundation on which we can begin to investigate the nature of orbits of the Koch snowflake billiard $\Omega(KS)$. We next describe the contents of this paper and outline our main results.

In order for the results of §§3–6 to be accessible to a broader audience, we provide in §2 a brief treatment of the necessary topics from the theory of mathematical billiards and particular examples from fractal geometry. In connection with mathematical billiards, we also give a brief description of how a flat surface can be used to rigorously relate the billiard flow on the billiard $\Omega(B)$, where B is a rational polygon, to the geodesic flow on the corresponding flat surface $\mathcal{S}(B)$.

The main results of the paper are presented in §§3–5. §3 contains results on the prefractal flat surface $\mathcal{S}(KS_n)$, for any arbitrary $n \geq 0$, and consequences of the fact (also established in §3, see Theorem 13) that such a surface is a branched cover of the hexagonal torus $\mathcal{S}(KS_0)$. Most importantly, we show that the billiard flow on the rational polygonal billiard $\Omega(KS_n)$ is dynamically equivalent to the geodesic flow on the associated prefractal flat surface $\mathcal{S}(KS_n)$. Such a result allows us to deduce that the set of directions for which a billiard orbit is closed (resp., dense) in $\Omega(KS_0)$ is exactly the set of directions for which an orbit is closed (resp., dense) in $\Omega(KS_n)$, for any $n \geq 0$. (See Theorem 15 and Corollary 16.)

This fact is used extensively in §4 when describing orbits of $\Omega(KS_n)$, $n \geq 0$, and constructing what we call a *sequence of compatible orbits*. Such a sequence consists

of orbits of each of the billiards $\Omega(KS_n)$, for $n = 0, 1, 2, ...$, with initial conditions that are themselves compatible in a suitable manner; see Definitions 20, 22, 23 and Remark 21. Using an addressing system developed in §2.4, we define what we are calling *hybrid orbits* of $\Omega(KS_n)$; see Definition 17. In a very concrete sense, hybrid orbits are orbits that mostly survive the construction of $\Omega(KS_{n+1})$ from $\Omega(KS_n)$. We show that dense orbits of $\Omega(KS_n)$ are actually dense *hybrid* orbits and we provide sufficient conditions under which a sequence of compatible orbits is a sequence of compatible periodic hybrid orbits. (See Proposition 19, along with Theorems 26 and 27.) In addition to this, we establish a *topological dichotomy* for sequences of compatible orbits: a sequence of compatible orbits is either entirely comprised of closed orbits or entirely comprised of dense hybrid orbits. (See Theorem 25.)

We would like to suggest that such sequences of compatible orbits should have suitable limits that constitute orbits of the Koch snowflake billiard. As we will see, there are hybrid orbits of $\Omega(KS_n)$ that remain fixed in every subsequent approximation $\Omega(KS_N)$, $n \geq N$, for some integer $N \geq 0$; see Theorem 30 and Example 31. Such hybrid orbits have basepoints corresponding to so-called *Cantor points* (i.e., points of KS which belong to some finite approximation KS_n but are not vertices of KS_n; see §2.5), and they certainly constitute periodic orbits of the Koch snowflake fractal billiard. In §5, a particular subset of basepoints can be derived from a certain sequence of compatible periodic hybrid orbits which is converging to a point of the snowflake curve called an *elusive limit point* (i.e., a point of KS which does not belong to any polygonal approximation KS_n, for $n \geq 0$; see §2.5). (An interesting example of such a situation is provided by a sequence of compatible 'hook orbits', discussed in Example 29; see also Example 28 further discussed in §5, as well as Conjecture 32.) Such basepoints can then be connected to form what we call a *nontrivial polygonal path* of $\Omega(KS)$. Furthermore, we consider the concatenation of two suitably chosen nontrivial polygonal paths, thereby connecting two elusive limit points of KS in a well-defined manner, as is done in §5.

In §6, since the field of "fractal billiards" is still in its infancy, we discuss directions for future research and provide several open questions and conjectures regarding the '*fractal flat surface*' $\mathcal{S}(KS)$ and the generalization of our results to other fractal tables. A number of these open questions are addressed in current works in progress (i.e., [14, 15]). For a more comprehensive, and somewhat different, list of conjectures, we refer the interested reader to [13, §6].

2. Background and preliminaries.

2.1. Mathematical billiards.
Under ideal conditions, we know that a point mass making a perfectly elastic collision with a C^1 surface (or curve) will reflect at an angle which is equal to the angle of incidence, this being referred to as the *law of reflection*.

Consider a compact region $\Omega(B)$ in the plane with connected boundary B. Then, $\Omega(B)$ is called a *planar billiard* when B is smooth enough to allow the law of reflection to hold, off of a set of measure zero (where the measure is taken to be the Hausdorff measure or the arc length measure). Though the law of reflection implicitly states that the angles of incidence and reflection be determined with respect to the normal to the line tangent at the basepoint, we adhere to the equivalent convention in the field of mathematical billiards that the vector describing the position and velocity of the billiard ball (which amounts to the position and angle, since we are assuming unit speed) be reflected in the tangent to the point of incidence. That
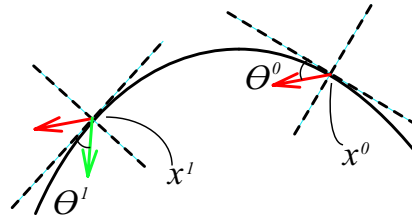
FIGURE 2. A billiard ball traverses the interior of a billiard and collides with the boundary. The velocity vector is pointed outward at the point of collision. The resulting direction of flow is found by either reflecting the vector through the tangent or by reflecting the incidence vector through the normal and reversing the direction of the vector. We use the former method in this paper.

is, employing such a law in order to determine the path on which the billiard ball departs after impact essentially amounts to identifying certain vectors.

Then we can rigorously reformulate the law of reflection as follows: the vector describing the direction of motion is the reflection—through the tangent at the point of collision—of the translation of the vector previously describing the direction of motion. One may express the law of reflection in terms of equivalence classes of vectors by identifying these two vectors to form an equivalence class of vectors in the unit tangent bundle corresponding to the billiard table $\Omega(B)$ (see Figure 2). (See [19] for a detailed discussion of this equivalence relation on the unit tangent bundle $\Omega(B) \times S^1$.)

The billiard map f_B is defined on the boundary B of the billiard table. Really, $f_B : (B \times S^1)/ \sim \to (B \times S^1)/ \sim$, where the equivalence relation $\sim$ is as discussed above. More precisely, if θ^0 is an inward pointing vector at a basepoint x^0, then (x^0, θ^0) is the representative element of the equivalence class $[(x^0, \theta^0)]$ and $f_B^k([x^0, \theta^0]) = [(x^k, \theta^k)]$, where $f_B^k := f_B \circ ... \circ f_B$ is the kth iterate of f_B.

When B is a nontrivial, connected polygon in $\mathbb{R}^2$, $\Omega(B)$ is called a *polygonal billiard*. The collection of vertices of $\Omega(B)$ forms a set of zero measure (when we take our measure to be the Hausdorff measure or simply, the arc-length measure on B), since there are finitely many vertices. A *rational billiard* is defined below.

Definition 1 (Rational polygon and rational billiard)**.** If B is a nontrivial connected polygon such that for each interior angle θ_j of B there are relatively prime integers $p_j \geq 1$ and $q_j \geq 1$ such that $\theta_j = \frac{p_j}{q_j}\pi$, then we call B a *rational polygon* and $\Omega(B)$ a *rational billiard*.

Remark 2. In the sequel, we will simply refer to an element $[(x^k, \theta^k)]$ by (x^k, θ^k), since the vector corresponding to θ^k is inward pointing at the basepoint x^k. So as not to introduce unneccessary notation, when we discuss the billiard map f_{KS_n} corresponding to the nth prefractal billiard $\Omega(KS_n)$, we will simply write f_{KS_n} as f_n. When discussing the discrete billiard flow on $(\Omega(KS_n) \times S^1)/ \sim$, the kth point in an orbit $(x^k, \theta^k) \in (\Omega(KS_n) \times S^1)/ \sim$ will instead be denoted by $(x_n^{k_n}, \theta_n^{k_n})$, so as to be clear as to which space such a point belongs. Specifically, k_n refers to the number of iterates of the billiard map f_n necessary to produce the pair $(x_n^{k_n}, \theta_n^{k_n})$. An initial condition of an orbit of $\Omega(KS_n)$ will always be referred to as (x_n^0, θ_n^0).

In the event that a basepoint x^j of $f_B^j(x^0, \theta^0)$ is a corner of $\Omega(B)$ (that is, a vertex of the polygonal boundary B), the resulting closed orbit is said to be *singular*. In addition, there exists a positive integer k such that the basepoint x^{-k} of $f_B^{-k}(x^0, \theta^0)$ is a corner of $\Omega(B)$. (Here, f_B^{-k} denotes the kth inverse iterate of f_B.) The path then traced out by the billiard ball connecting x^j and x^{-k} is called a *saddle connection*.

Definition 3 (Footprint of an orbit). Let $\mathscr{O}_n(x_n^0, \theta_n^0)$ be an orbit of $\Omega(KS_n)$. Then

$$\mathcal{F}_n(x_n^0, \theta_n^0) := \mathscr{O}_n(x_n^0, \theta_n^0) \cap KS_n \tag{1}$$

is called the *footprint* of the orbit $\Omega(KS_n)$.

2.2. **Flat surfaces and properties of the flow.** In this section, we deal only with flat surfaces constructed from rational billiards.

Definition 4 (Flat structure and flat surface). Let M be a compact, connected, orientable surface. A *flat structure* on M is an atlas ω, consisting of charts of the form $(U_\alpha, \varphi_\alpha)_{\alpha \in \mathscr{A}}$, where U_α is a domain (i.e., a connected open set) in M and φ_α is a homeomorphism from U_α to a domain in $\mathbb{R}^2$, such that the following conditions hold:

1. the collection $\{U_\alpha\}_{\alpha \in \mathscr{A}}$ cover the whole surface M except for finitely many points $z_1, z_2, ..., z_k$, called *singular points*;
2. all coordinate changing functions are translations in $\mathbb{R}^2$;
3. the atlas ω is maximal with respect to properties (1) and (2);
4. for each singular point z_j, there is a positive integer m_j, a punctured neighborhood $\dot{U}_j$ of z_j not containing other singular points, and a map ψ_j from this neighborhood to a punctured neighborhood $\dot{V}_j$ of a point in $\mathbb{R}^2$ that is a shift in the local coordinates from ω, and is such that each point in $\dot{V}_j$ has exactly m_j preimages under ψ_j.

We say that a connected, compact surface equipped with a flat structure is a *flat surface*.

Remark 5. Note that in the literature on billiards and dynamical systems, the terminology and definitions pertaining to this topic are not completely uniform; see, for example, [4, 5, 7, 8, 10, 9, 17, 18, 22, 23, 24, 26]. We have adopted the above definition for clarity and the reader's convenience.

We now discuss how to construct a flat surface from a rational billiard. Consider a rational polygon billiard $\Omega(P)$ with k sides and interior angles $\frac{p_j}{q_j}\pi$ at each vertex z_j, for $1 \leq j \leq k$, where the positive integers p_j and q_j are relatively prime. The linear portions of the planar symmetries generated by reflection in the sides of the polygonal billiard $\Omega(P)$ generate the dihedral group D_N, where $N := \mathrm{lcm}\{q_j\}_{j=1}^k$. Next, we consider $\Omega(P) \times D_N$ (equipped with the product topology). We want to glue 'sides' of $\Omega(P) \times D_N$ together and construct a natural atlas on the resulting surface M so that M becomes a flat surface.

As a result of the identification, the points of M that correspond to the vertices of $\Omega(P)$ constitute (removable or nonremovable) conic singularities of this surface. Heuristically, $\Omega(P) \times D_N$ can be represented as $\{r_j\Omega(P)\}_{j=1}^{2N}$, in which case it is easy to see what sides are made equivalent under the action of $\sim$. That is, $\sim$ identifies opposite and parallel sides in a manner which preserves the orientation.
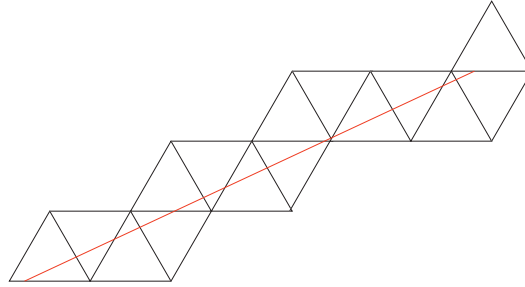
FIGURE 3. Unfolding an orbit of the equilateral triangle billiard $\Omega(KS_0)$.

2.3. **Unfolding a billiard orbit.** Consider a rational polygonal billiard $\Omega(B)$ and an orbit $\mathcal{O}(x^0, \theta^0)$. Reflecting the billiard $\Omega(B)$ and the orbit in a side of the billiard containing a basepoint of the orbit (or an element of the footprint of the orbit) partially unfolds the orbit $\mathcal{O}(x^0, \theta^0)$; see Figure 3. Continuing this process until the orbit is a straight line produces as many copies of the billiard table as there are elements of the footprint. That is, if the period of an orbit $\mathcal{O}(x^0, \theta^0)$ is some positive integer p, then the number of copies of the billiard table in the unfolding is also p. Therefore, we refer to such a straight line as the unfolding of the billiard orbit.

2.4. **Symbolic representation of the ternary Cantor set.** Every point of the ternary Cantor set $\mathscr{C}$ (hereafter referred to as the Cantor set) has a ternary *representation* given in terms of the characters l, c and r (standing for left, center and right, respectively). For example, in terms of our alphabet, we say $1/3$ has a ternary representation given by $l\overline{r}$ and $1/4$ has a ternary representation given by $\overline{lr}$, where the over-bar indicates that the corresponding string of symbols is repeated ad infinitum. We stress that a ternary *representation* will always consist of infinitely many characters, while a ternary *expansion* of an element of the unit interval I can be finite, which is illustrated by the example of the rational value $1/3 = 0.1$ in base-3. For the sake of simplicity, we take every element of $\mathscr{C}$ to have a ternary representation that contains no c's. (What we want to prevent is an element of $\mathscr{C}$ having a representation determined by approaching it from the complement of $\mathscr{C}$ in $I = [0, 1]$. In this way, every point of $\mathscr{C}$ has a unique ternary representation.)

In the sequel, the *type* of ternary representation will provide us with important information. Particular qualities of the representation will, in part, dictate the type of resulting orbit and the nature of the sequence of compatible orbits.

Notation 6. The *type of ternary representation* can be defined as follows. If $x \in I$, then the first coordinate of $[\cdot, \cdot]$ describes the characters that occur infinitely often and the second coordinate of $[\cdot, \cdot]$ describes the characters that occur finitely often. If we want to discuss many different types of ternary representations, then we use 'or.' That is, the notation $[\cdot, \cdot] \vee [\cdot, \cdot] \vee ... \vee [\cdot, \cdot]$ is to be read as $[\cdot, \cdot]$ *or* $[\cdot, \cdot]$ *or ... or* $[\cdot, \cdot]$. If the collection of characters occurring finitely often is empty, then we denote the corresponding type of ternary representation by $[\cdot, \emptyset]$.

Example 7. If an element $x \in I = [0, 1]$ has a ternary representation consisting of infinitely many c's and l's but finitely many r's, then we write this type of ternary representation as $[lc, r]$. If we have a collection of points in I such that each point
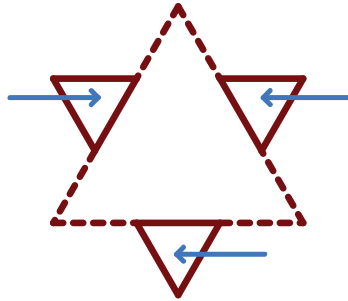
FIGURE 4. An illustration of Definition 8 in terms of $KS_0 = \Delta$ and KS_1. Represented are the three cells $C_{1,1}$, $C_{1,2}$ and $C_{1,3}$ of $\Omega(KS_1)$.

has a ternary representation consisting of infinitely many c's and l's and finitely many r's or else infinitely many l's and r's and finitely many c's, then we write the corresponding types of ternary representations as $[lc, r] \vee [lr, c]$.

2.5. The Koch snowflake. The Koch snowflake KS is a compact, connected and infinitely long curve in the plane with the property that at no point of the snowflake KS can one form a well-defined tangent. This last property is what makes defining a law of reflection on the Koch snowflake billiard boundary so difficult.

The Koch snowflake is constructed, as shown in Figure 1, by removing the open middle third of each successive side of length $1/3^{n-1}$ and placing at each pair of endpoints two uprights that would have formed the sides of an equilateral triangle with side lengths measuring $1/3^n$.

Next, we define what a *cell* of the Koch snowflake billiard is.

Definition 8 (A cell $C_{n,\nu}$ of $\Omega(KS_n)$)**.** Consider (the 'set-theoretic difference') $\Omega(KS_n) \backslash \Omega(KS_{n-1})$. Each resulting triangular region is then called a *cell* of $\Omega(KS_n)$. We denote a cell of $\Omega(KS_n)$ by $C_{n,\nu}$, where ν denotes the side of $\Omega(KS_{n-1})$ to which the cell was glued; see Figure 4. Hence, there are $3 \cdot 4^{n-1}$ cells $C_{n,\nu}$ of $\Omega(KS_n)$ and so $1 \leq \nu \leq 3 \cdot 4^{n-1}$.

In §4, we will be interested in the information provided by the ternary representation of an element x_n^0 of a side $s_{n,\nu}$ of $\Omega(KS_n)$. We have already seen how to represent elements of the unit interval I. An element of a side $s_{n,\nu}$ of $\Omega(KS_n)$ has a ternary representation also given in terms of the characters l, c and r.

In the Koch snowflake KS, there are three types of points: *corners, Cantor points* and *elusive limit points*. A *corner* of the Koch snowflake KS is a point of KS that is a corner of a finite approximation KS_n, for some $n \geq 0$. A *Cantor point* of KS is a point of a finite approximation KS_n, for some $n \geq 0$, such that the ternary representation of this point (with respect to the side on which it lies) has the form $[lr, \emptyset]$ (that is, consists of infinitely many l's *and* r's and no c's). Therefore, a Cantor point is a point of KS that is not a corner, but definitely a point of KS that exists in some finite approximation KS_n. An *elusive limit point* of KS is a point of KS that never belongs to any finite approximation KS_n. We will see that it is the Cantor points and elusive limit points that will be of the greatest interest in the sequel.

3. The Koch snowflake prefractal flat surface $\mathcal{S}(KS_n)$. We denote by $\mathcal{S}(P)$ the flat surface M constructed from a particular rational billiard $\Omega(P)$.
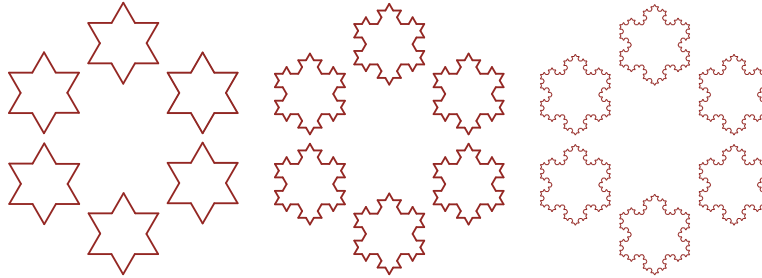
FIGURE 5. The flat surfaces $\mathcal{S}(KS_n)$, for $n = 1, 2, 3$. Note that the proper identification is not shown in the figures above. Given the arrangement of the six copies of KS_n, one then identifies opposite and parallel sides to make the proper identification that results in a geodesic flow that is dynamically equivalent with the billiard flow on the associated billiards $\Omega(KS_1), \Omega(KS_2), \Omega(KS_3)$.

In particular, $\mathcal{S}(KS_n)$ is the flat surface associated with the prefractal billiard $\Omega(KS_n)$. The flat surfaces $\mathcal{S}(KS_n)$, $n = 1, 2, 3$, are given in Figure 5. For each billiard $\Omega(KS_n)$, the group of symmetries D_N, where $N = \mathrm{lcm}\{q_j\}_{j=1}^{3 \cdot 4^n}$ (that is, the second component in the product $\Omega(KS_n) \times D_N$) is the dihedral group D_3, and thus is independent of n. From this, we deduce that for any $n \geq 0$, there are six copies of the prefractal billiard table $\Omega(KS_n)$ (with sides appropriately identified) used in the construction of the associated flat surface $\mathcal{S}(KS_n) := (\Omega(KS_n) \times D_3)/\sim$; see Figure 5. We refer the reader back to §2.2 for a general discussion of flat surfaces and, e.g., to [16] for the topological notions (such as covering map, branched cover) used in this section (esp., in Theorem 13 and its proof).

Remark 9. For the remainder of the paper, when we say that a regular polygon is of *scale* n, we mean that the side length of the regular polygon is $1/3^n$. For example, an equilateral triangle of scale n is one for which the side length is $1/3^n$.

The flat surface $\mathcal{S}(KS_n)$ is a surface with both types of conic singularities: removable and nonremovable. In constructing the flat surface $\mathcal{S}(KS_n)$ via $\Omega(KS_n)$, we see that the nonremovable conic singularities correspond to corners with obtuse angles of $\Omega(KS_n)$ and removable singularities correspond to corners with acute angles (both measured relative to the interior of $\Omega(KS_n)$). Since for every $n \geq 1$, the measure of every obtuse corner is the same (specifically, $4\pi/3$ radians), it follows that the conic angle of a nonremovable singularity is 8π. For the same reason, every corner with an acute angle (with every acute angle measuring $\pi/3$ radians) gives rise to a removable singularity with conic angle 2π; this is, in fact, a defining characteristic of a removable singularity.

Proposition 10. *For any $n \geq 0$, the genus g_n of the surface $\mathcal{S}(KS_n)$ is given by*

$$g_n = 3 \cdot 4^n - 2. \tag{2}$$

Proof. Let $\Omega(P)$ be a rational billiard and let $\{V_j\}_{j=1}^{\nu}$ denote the ν vertices of the polygon P. For each $j = 1, ..., \nu$, let the measure of the angle formed by the vertex V_j be $(p_j/q_j)\pi$, and let $N := \mathrm{lcm}\{q_j\}_{j=1}^{\nu}$. Then, if g is the genus of the corresponding flat surface $\mathcal{S}(P)$, the Euler characteristic $\chi = 2 - 2g$ of that same
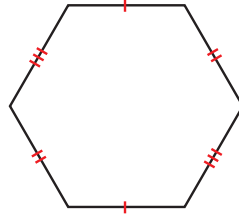
FIGURE 6. The hexagonal torus $\mathcal{S}(KS_0)$. As usual, similarly marked sides are identified. It should be noted that $\mathcal{S}(KS_0)$ is topologically (but not metrically) equivalent to the flat square torus.

surface is given by

$$\chi = N \sum_{j=1}^{\nu} \frac{1}{q_j} - N\nu + 2N; \tag{3}$$

see [9] for a detailed description of how to calculate the genus of a surface that arises from a rational billiard table.

The prefractal billiard $\Omega(KS_n)$ has $3 \cdot 4^n$ many sides and as many vertices. Moroever, $N_n = \operatorname{lcm}\{q_j\}_{j=1}^{3 \cdot 4^n} = 3$, for every $n \geq 0$. The Euler characteristic $\chi_n = 2 - 2g_n$ of $\mathcal{S}(KS_n)$ is given by Equation (3). Therefore, solving for g_n, we see that the genus of the prefractal flat surface $\mathcal{S}(KS_n)$ is given by Equation (2). □

3.1. $\mathcal{S}(KS_n)$ **is a branched cover of** $\mathcal{S}(KS_0)$. Taking as inspiration the results and methods of Gutkin and Judge in [7] and [8], we now show that for each $n \geq 1$, the flat surface $\mathcal{S}(KS_n)$ is a branched cover of the hexagonal torus $\mathcal{S}(KS_0)$; see Figure 6. To such end, we establish several results culminating in this fact.

Lemma 11. *Let $n \in \mathbb{N}$. Then, for any positive integer $k \geq n$, $\mathcal{S}(KS_n)$ can be tiled by equilateral triangles of scale k.*

Proof. This follows from the construction of the Koch snowflake. We note that each triangle of scale n, denoted Δ_n, can be tiled by 9^{k-n} triangles of scale $k \geq n$; see Figure 7 for the case when $k = n+1$. Note that $\mathcal{S}(KS_n) = (\Omega(KS_n) \times D_3)/\sim$ and that $\Omega(KS_n)$ is constructed from $\Omega(KS_{n-1})$ by gluing a copy of Δ_n to every side $s_{n-1,\nu}$ at the middle third of $s_{n-1,\nu}$. Since every triangle Δ_{n-1} tiling $\Omega(KS_{n-1})$ can also be tiled by Δ_n, it follows that $\Omega(KS_n)$ is tiled by Δ_n. So, $\mathcal{S}(KS_n)$ can be tiled by equilateral triangles of scale k, for every $k \geq n$. □

In the sequel, given a bounded set $A \subseteq \mathbb{R}^2$, we will write that "A can be tiled by H_n" in order to indicate that A can be tiled by finitely many copies of hexagonal tiles H_n of scale n.

Proposition 12. *Let $n \in \mathbb{N}$. Then the flat surface $\mathcal{S}(KS_n)$ can be tiled by H_k, for all $k \geq n+1$, in such a way that each conic singularity is at the center of some tile H_k.*

Proof. We see in Figure 8 that $\mathcal{S}(KS_1)$ can be tiled by H_2 such that each conic singularity is at the center of some tile H_2. Each H_2 is tiled by six equilateral triangles Δ_2. As was seen in the proof of Lemma 11, each Δ_2 is tiled by nine Δ_3 such that six of these triangles form a hexagonal tile H_3; see Figure 7. At the center
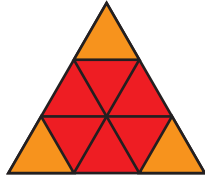
FIGURE 7. We see that Δ_n is tiled by nine copies of Δ_{n+1}, six of
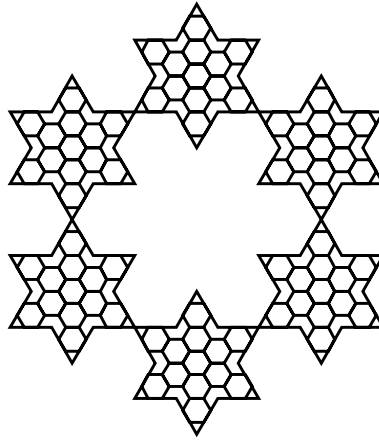which form a hexagonal tile H_{n+1} in the center.

FIGURE 8. Tiling the flat surface $\mathcal{S}(KS_1)$ by hexagonal tiles H_2.
We note that the conic singularities (both removable and nonre-
movable) are at the center of hexagonal tiles.

of H_2 is a copy of H_3. Hence, each conic singularity remains at the center of some
tile H_3; see Figure 9. Continuing in this fashion, we see that for each $k \geq 2$, H_k
tiles $\mathcal{S}(KS_2)$ in such a way that each conic singularity is at the center of some H_k.

Suppose there exists $N \in \mathbb{N}$ such that, for every $n \leq N$, $\mathcal{S}(KS_n)$ can be tiled
by H_k, for every $k \geq n + 1$. In particular, $\mathcal{S}(KS_N)$ can be tiled by H_k, for every
$k \geq N + 1$. We then have that, for every $k \geq N + 2$, $\mathcal{S}(KS_N)$ can be tiled by H_k.
By Lemma 11, Δ_{N+1} tiles $\mathcal{S}(KS_{N+1})$. Each triangular region Δ_{N+1} in $\mathcal{S}(KS_{N+1})$
but not in $\mathcal{S}(KS_N)$ is tiled by nine triangles Δ_{N+2} in such a way that six Δ_{N+2}
comprise a tile H_{N+2}. Continuing in this fashion, we see that each Δ_k contributes
to a hexagonal tile H_k (as part of the embedded tiling) in such a way that each
conic singularity is at the center of some hexagonal tile H_k. $\square$

Theorem 13. *For every $n \in \mathbb{N}$, the prefractal Koch snowflake flat surface $\mathcal{S}(KS_n)$
is a branched cover of the (singly punctured) prefractal Koch snowflake flat surface
$\mathcal{S}(KS_0)$, which is the hexagonal torus. Such a covering map $p_n : \mathcal{S}(KS_n) \to \mathcal{S}(KS_0)$
is given by suitably defined translations on $\mathcal{S}(KS_n)$.*

Proof. The center point x_0 of the flat hexagonal torus $\mathcal{S}(KS_0)$ is a branched locus
of the cover $\mathcal{S}(KS_n)$ when $\mathcal{S}(KS_n)$ is tiled by H_{n+1} as described in Proposition 12.
This follows from the fact that every nonremovable conic singularity of $\mathcal{S}(KS_n)$ is
at the center of four hexagonal tiles. Specifically, this means that this center point
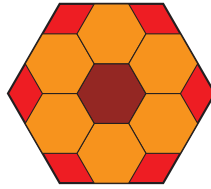x_0 is not evenly covered by the covering map $p_n : \mathcal{S}(KS_n) \to \mathcal{S}(KS_0)$ determined

FIGURE 9. Six triangles Δ_n tile H_n. The hexagonal tile H_n is tiled by seven tiles H_{n+1} with six rhombic tiles.
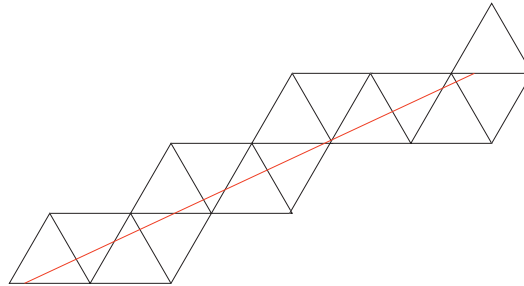

FIGURE 10. The lattice points constitute linear integer combinations of the basis vectors $\{u_1, u_2\} = \{(1,0), (1/2, \sqrt{3}/2)\}$. Here we show an unfolded orbit to emphasize the utility of such a tool. The unfolded orbit has an initial direction that is rational, meaning such an orbit will be closed in the equilateral triangle.

by suitable translations of hexagonal tiles H_{n+1} on $\mathcal{S}(KS_n)$. Any other point in $\mathcal{S}(KS_0)$ is evenly covered since every element in the fiber $p_n^{-1}(z)$, $z \neq x_0$, has a conic angle of 2π. $\qquad\square$

3.2. **Minimality of the flow on $\Omega(KS_n)$ and its consequences.** When discussing billiard orbits of $\Omega(KS_n)$, we will find it more convenient to measure angles of incidence and reflection relative to a fixed coordinate system. As such, we suppose that the left corner of the equilateral triangle with side length one constitutes the origin. However, on occasion, we will find it useful to refer to the angle of reflection measured relative to a particular side. So that no confusion arises, when we are discussing such a situation, if ϖ is an angle measured relative to a side of $\Omega(KS_n)$, then $\theta(\varpi)$ is the same angle measured relative to the fixed coordinate system.

If $\{u_1, u_2\}$ is a basis for $\mathbb{R}^2$, then a vector $z \in \mathbb{R}^2$ is called *rational with respect to* $\{u_1, u_2\}$ if $z = mu_1 + nu_2$, for some $m, n \in \mathbb{Z}$. Combining the results of [7] with Theorem 3 of [6], we can state the following result, which we do not claim as a new theorem, but which we rephrase in a way that is suitable for our purposes.

Theorem 14 ([6]). *Let $\mathcal{S}(P)$ be a flat surface determined from a rational polygonal billiard $\Omega(P)$. If $\mathcal{S}(P)$ is a branched cover of a singly punctured torus, then a geodesic on $\mathcal{S}(P)$ is periodic or forms a saddle connection if and only if the geodesic has an initial direction that is rational. In addition, a geodesic on $\mathcal{S}(P)$ is dense if and only if the geodesic has an initial direction that is irrational.*

By what we saw in §§2.2 and 2.3, the geodesic flow on $\mathcal{S}(KS_n)$ is dynamically equivalent to the billiard flow on $\Omega(KS_n)$. In §3.1, we proved that $\mathcal{S}(KS_n)$ is a

branched cover of the singly punctured torus $\mathcal{S}(KS_0)$. Applying Theorem 14 to the Koch snowflake prefractal flat surfaces, we then obtain the following result.

Theorem 15. *Let $n \geq 0$. A direction θ is a rational direction (with respect to the basis $\{u_1, u_2\} = \{(1,0), (1/2, \sqrt{3}/2)\}$) if and only if a geodesic in the direction of θ on $\mathcal{S}(KS_n)$ is periodic or forms a saddle connection. Furthermore, a direction θ is an irrational direction (with respect to $\{u_1, u_2\}$) if and only if a geodesic in the direction of θ on $\mathcal{S}(KS_n)$ is dense.*

Because the geodesic flow on the prefractal flat surface $\mathcal{S}(KS_n)$ is dynamically equivalent to the billiard flow on the corresponding billiard table $\Omega(KS_n)$, we can state Theorem 15 in terms of the billiard flow on the prefractal billiard $\Omega(KS_n)$.

Corollary 16. *Let $n \geq 0$. A direction θ is a rational direction (with respect to $\{u_1, u_2\} = \{(1,0), (1/2, \sqrt{3}/2)\}$) if and only if an orbit in the direction of θ of $\Omega(KS_n)$ is closed. Furthermore, a direction θ is an irrational direction (with respect to $\{u_1, u_2\}$) if and only if an orbit with the initial direction of θ in $\Omega(KS_n)$ is dense.*

4. **Hybrid orbits of the Koch snowflake prefractal billiard $\Omega(KS_n)$.** We want to construct sequences of orbits in such a way that one orbit is suitably related to another. More precisely, we want to develop a notion of 'compatibility' that relates an orbit of $\Omega(KS_n)$ to an orbit of $\Omega(KS_{n+1})$, for each $n \geq 0$. Let us first consider an orbit of $\Omega(KS_0)$. Such an orbit has basepoints that potentially lie on segments that are removed as part of the construction of finer prefractal approximations, on the Cantor set that remains as part of the construction process or both. Obviously, an orbit of $\Omega(KS_0)$ may not be an orbit of $\Omega(KS_1)$.[1] However, depending on the types of the ternary representations of the basepoints of the orbit of $\Omega(KS_0)$, a sequence of compatible orbits will exhibit particularly interesting dynamical behavior. While certain orbits in a so-called sequence of compatible orbits will form saddle connections in their respective billiard tables, we will see that this is the exception rather than the rule.

A hybrid orbit of a prefractal billiard is an orbit of $\Omega(KS_n)$ for which the elements of the corresponding footprint are such that they correspond to at most two points of KS with finite ternary expansions (i.e., corners). As we will see, certain orbits remain constant from one prefractal billiard $\Omega(KS_n)$ to the next and certain orbits change entirely with each prefractal billiard approximation. The term *hybrid* is meant to indicate that such orbits have qualities that are found in these two types of orbits mentioned in the previous sentence. As such, Definition 17 is phrased so as to include these two types of orbits and more general orbits that have qualities reminiscent of both. The motivation for defining such an orbit comes from the fact that we are interested in the situation where a periodic orbit is an element in a sequence of orbits, where each orbit in the sequence is also a periodic orbit.

We are further motivated in our definition of a hybrid orbit based on Theorem 26, which states that if $\mathcal{O}_0(x_0^0, \theta_0^0)$ is a periodic hybrid orbit of $\Omega(KS_0)$ and no basepoints of the orbit correspond to ternary points of KS_0, then, for every $n \geq 0$, the *compatible orbit* $\mathcal{O}_n(x_n^0, \theta_n^0)$ (see Definitions 20, 22, 23 and Remark 21) will be a periodic hybrid orbit of $\Omega(KS_n)$. In general, knowing whether or not an orbit $\mathcal{O}_N(x_N^0, \theta_N^0)$ is a dense orbit or a closed orbit will be sufficient for determining a

---

[1]See Figure 11 and the corresponding caption, as well as the discussion preceding Definition 20 for an example illustrating the situation where basepoints of an orbit $\mathcal{O}_0(x_0^0, \theta_0^0)$ lie on segments of $\Omega(KS_0)$ that are removed in the construction of $\Omega(KS_1)$.

topological dichotomy for a sequence of compatible orbits $\{\mathscr{O}_n(x_n^0, \theta^0)\}_{n=N}^{\infty}$; see Definition 23 and Theorem 25. To such end, we begin by defining a hybrid orbit below.

Definition 17 (Hybrid orbit). Let $\mathscr{O}_n(x_n^0, \theta_n^0)$ be an orbit of $\Omega(KS_n)$. If all but at most two basepoints $x_n^{k_n} \in \mathcal{F}_n(x_n^0, \theta_n^0)$ have ternary representations (determined with respect to the side $s_{n,\nu}$ on which each point resides) of type $[c, lr] \vee [cl, r] \vee [cr, l] \vee [lcr, \emptyset] \vee [lr, \emptyset]$, then we call $\mathscr{O}_n(x_n^0, \theta_n^0)$ a *hybrid orbit* of $\Omega(KS_n)$.

Definition 18 (A $\mathscr{P}$ hybrid orbit). If $\mathscr{O}_n(x_n^0, \theta_n^0)$ is a hybrid orbit with property $\mathscr{P}$, then we say that it is a $\mathscr{P}$ hybrid orbit.

Proposition 19. *If $\mathscr{O}_n(x_n^0, \theta_n^0)$ is a dense orbit of $\Omega(KS_n)$, then $\mathscr{O}_n(x_n^0, \theta_n^0)$ is a dense hybrid orbit.*

Proof. Suppose there were two basepoints $x_n^{k_n}$ and $x_n^{k_n'}$ of a dense orbit $\mathscr{O}_n(x_n^0, \theta_n^0)$ with ternary representations of types $[l, cr] \vee [r, lc]$. Then, there exists $N \geq n$ such that the orbit connects two vertices of two equilateral triangles of scale N tiling $\Omega(KS_n)$. Since this orbit can be unfolded (much as in §2.3) into the corresponding flat surface and then projected down onto the hexagonal torus, such an orbit (or flow line on the flat surface) must be at least a saddle connection of the equilateral triangle billiard. However, such a direction θ_n^0 should yield a dense billiard flow in $\Omega(KS_0)$, which is not the case. Hence, $x_n^{k_n}$ and $x_n^{k_n'}$ do not both have a ternary representation of type $[l, cr] \vee [r, lc]$. Moreover, if any basepoint of $\mathscr{O}_n(x_n^0, \theta_n^0)$ already corresponds to a corner of $\Omega(KS_n)$, then a similar argument shows that no other basepoint may have a ternary representation of type $[l, cr] \vee [r, lc]$. Therefore, $\mathscr{O}_n(x_n^0, \theta_n^0)$ is a dense hybrid orbit. $\square$

Beginning with Definition 20, we will construct a framework for handling the Koch snowflake billiard $\Omega(KS)$, part of which has been referred to at the beginning of this section. In particular, we will define a specific type of sequence of orbits of prefractal approximations, and examine various properties of such a sequence of orbits. To motivate the following definitions, we examine a particular orbit $\mathscr{O}_0(x_0^0, \theta_0^0)$ of $\Omega(KS_0)$ and the consequences for the orbit when constructing $\Omega(KS_1)$ from $\Omega(KS_0)$. In Figure 11, we see an example of an orbit $\mathscr{O}_0(x_0^0, \theta_0^0)$ with basepoints lying on segments of the boundary of $\Omega(KS_0)$ that are removed as part of the construction of $\Omega(KS_1)$ from $\Omega(KS_0)$. Consequently, the orbit $\mathscr{O}_0(x_0^0, \theta_0^0)$ is no longer an orbit of $\Omega(KS_1)$, since the basepoints of the orbit lie in the interior of $\Omega(KS_1)$. The third image in Figure 11 shows an orbit $\mathscr{O}_1(x_1^0, \theta_1^0)$ with the property that x_0^0 (now a point in the interior of $\Omega(KS_1)$) and x_1^0 are collinear in the direction determined by θ_0^0 (which, by construction, is equal to θ_1^0). As we will see, the two initial conditions (x_0^0, θ_0^0) and (x_1^0, θ_1^0) are what we call *compatible initial conditions*. We then build upon the definition of compatible initial conditions to construct what we call a *sequence of compatible initial conditions* and, subsequently, a *sequence of compatible orbits*. It is in this way that we will be able to investigate the behavior of what we call *nontrivial polygonal paths* in §5. We continue with the following definition.

Definition 20 (Compatible initial conditions). Without loss of generality, suppose that n and m are nonnegative integers such that $n > m$. Let $(x_n^0, \theta_n^0) \in (KS_n \times S^1)/\sim$ and $(x_m^0, \theta_m^0) \in (KS_m \times S^1)/\sim$ be two initial conditions of the orbits $\mathscr{O}_n(x_n^0, \theta_n^0)$ and $\mathscr{O}_m(x_m^0, \theta_m^0)$, respectively, where we are assuming that θ_n^0 and θ_m^0
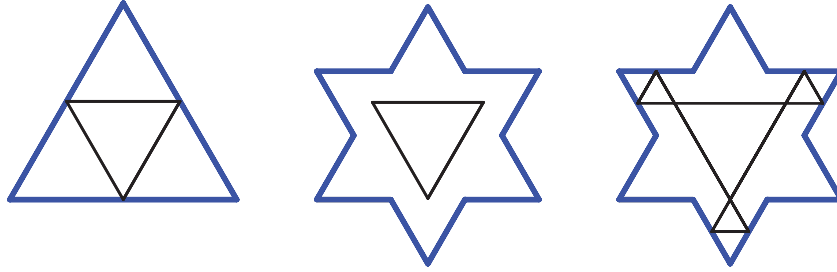
FIGURE 11. In this figure, we see that an orbit $\mathcal{O}_0(x_0^0, \theta_0^0)$ of $\Omega(KS_0)$ need not be an orbit of $\Omega(KS_1)$. Upon removing segments and constructing $\Omega(KS_1)$ from $\Omega(KS_0)$, the basepoints of the orbit become points of the interior of $\Omega(KS_1)$. However, we can construct an orbit $\mathcal{O}_1(x_1^0, \theta_1^0)$ of $\Omega(KS_1)$ that is *compatible* with $\mathcal{O}_0(x_0^0, \theta_0^0)$ in the sense discussed in Remark 21.

are both inward pointing. If $\theta_n^0 = \theta_m^0$ and if x_n^0 and x_m^0 lie on a segment determined from θ_n^0 (or θ_m^0) that intersects KS_n only at x_n^0, then we say that (x_n^0, θ_n^0) and (x_m^0, θ_m^0) are *compatible initial conditions*.

Remark 21. When two initial conditions (x_n^0, θ_n^0) and (x_m^0, θ_m^0) are compatible, then we simply write each as (x_n^0, θ^0) and (x_m^0, θ^0). If two orbits $\mathcal{O}_m(x_m^0, \theta_m^0)$ and $\mathcal{O}_n(x_n^0, \theta_n^0)$ have compatible initial conditions, then we say that such orbits are *compatible*.

Not every orbit must pass through the region of $\Omega(KS_n)$ corresponding to the interior of $\Omega(KS_0)$, let alone pass through the interior of $\Omega(KS_m)$, for any $m < n$. Because of this, it may be the case that an initial condition (x_n^0, θ^0) is not compatible with (x_m^0, θ^0), for any $m < n$.

Definition 22 (Sequence of compatible initial conditions). Let $\{(x_i^0, \theta_i^0)\}_{i=N}^\infty$ be a sequence of initial conditions, for some integer $N \geq 0$. We say that this sequence is a *sequence of compatible initial conditions* if for every $m \geq N$ and for every $n > m$, we have that (x_n^0, θ_n^0) and (x_m^0, θ_m^0) are compatible initial conditions. In such a case, we then write the sequence as $\{(x_i^0, \theta^0)\}_{i=N}^\infty$.

Definition 23 (Sequence of compatible orbits). Consider a sequence of compatible initial conditions $\{(x_n^0, \theta^0)\}_{n=N}^\infty$. Then the corresponding sequence of orbits $\{\mathcal{O}_n(x_n^0, \theta^0)\}_{n=N}^\infty$ is called *a sequence of compatible orbits*.

If $\mathcal{O}_m(y_m^0, \theta(\varpi_m^0))$ is an orbit of $\Omega(KS_m)$, then $\mathcal{O}_m(y_m^0, \theta(\varpi_m^0))$ is a member of a sequence of compatible orbits $\{\mathcal{O}_n(x_n^0, \varpi^0)\}_{n=N}^\infty$ for some $N \geq 0$. It is clear from the definition of a sequence of compatible orbits that such a sequence is determined by the first orbit $\mathcal{O}_N(x_N^0, \varpi^0)$. Since the initial condition of an orbit determines the orbit, we can say without any ambiguity that a sequence of compatible orbits is determined by an initial condition (x_N^0, ϖ^0).

Definition 24 (A sequence of compatible $\mathcal{P}$ orbits). Let $\mathcal{P}$ be a property (resp., $\mathcal{P}_1, ..., \mathcal{P}_j$ a list of properties). If every orbit in a sequence of compatible orbits has the property $\mathcal{P}$ (resp., a list of properties $\mathcal{P}_1, ..., \mathcal{P}_j$), then we call such a sequence *a sequence of compatible $\mathcal{P}$ (resp., $\mathcal{P}_1, ..., \mathcal{P}_j$) orbits*.

We know that for each fixed billiard table $\Omega(KS_n)$ and fixed direction θ_n^0, an orbit is either closed or dense, regardless of the initial basepoint x_n^0. Applying the results in §§3.1 and 3.2, we have the following.

Theorem 25 (A topological dichotomy for sequences of compatible orbits). *Let* $\{\mathscr{O}_n(x_n^0, \theta^0)\}_{n=N}^{\infty}$ *be a sequence of compatible orbits. Then* $\{\mathscr{O}_n(x_n^0, \theta^0)\}_{n=N}^{\infty}$ *is either entirely comprised of closed orbits or is entirely comprised of dense hybrid orbits.*

Proof. Let $\{\mathscr{O}_n(x_n^0, \theta^0)\}_{n=N}^{\infty}$ be a sequence of compatible orbits. By construction θ^0 is the same initial direction for every orbit in the sequence of compatible orbits. Suppose θ^0 is rational with respect to the basis $\{u_1, u_2\} := \{(1,0), (1/2, \sqrt{3}/2)\}$. Then, applying Corollary 16, for every $n \geq N$, we deduce that the orbit $\mathscr{O}_n(x_n^0, \theta^0)$ is a closed orbit of $\Omega(KS_n)$. Hence, $\{\mathscr{O}_n(x_n^0, \theta^0)\}_{n=N}^{\infty}$ is a sequence of compatible orbits for which every orbit in the sequence is closed.

Suppose now that θ^0 is irrational with respect to the basis $\{u_1, u_2\}$. Then, by Corollary 16, for every $n \geq N$, the orbit $\mathscr{O}_n(x_n^0, \theta_n^0)$ is a dense orbit of $\Omega(KS_n)$. By Proposition 19, $\mathscr{O}_n(x_n^0, \theta_n^0)$ is therefore a dense hybrid orbit of $\Omega(KS_n)$. Hence, $\{\mathscr{O}_n(x_n^0, \theta^0)\}_{n=N}^{\infty}$ is a sequence of compatible orbits for which every orbit in the sequence is a dense hybrid orbit. $\qquad\square$

Theorem 26. *If* $\mathscr{O}_0(x_0^0, \theta_0^0)$ *is a periodic hybrid orbit of* $\Omega(KS_0)$ *with no basepoints corresponding to ternary points, then for every* $n \geq 0$, *the compatible orbit* $\mathscr{O}_n(x_n^0, \theta_n^0)$ *is a periodic hybrid orbit of* $\Omega(KS_n)$.

Proof. Since $\Omega(KS_n)$ can be tiled by scale n copies of $\Omega(KS_0)$, an orbit of $\Omega(KS_0)$ can be unfolded in the Koch snowflake prefractal billiard $\Omega(KS_n)$, for every $n \geq 0$; see §2.3. Therefore, each basepoint of the corresponding compatible orbit $\mathscr{O}_n(x_n^0, \theta_n^0)$ will have a ternary representation consistent with that described in Definition 17. $\qquad\square$

Theorem 27 (A sequence of compatible periodic hybrid orbits). *Consider a vector* (a, b) *that is rational with respect to the basis* $\{u_1, u_2\} := \{(1,0), (1/2, \sqrt{3}/2)\}$ *and let* $x_0^0 \in I$. *Then, we have the following*:

1. *If* a *and* b *are both positive integers with* b *being odd,* $x_0^0 = \frac{r}{4^s}$, *for some* $r, s \in \mathbb{N}$ *with* $s \geq 1$, $1 \leq r < 4^s$ *being odd and* $\theta^0 := \arctan\frac{b\sqrt{3}}{2a+b}$, *then the sequence of compatible closed orbits* $\{\mathscr{O}_n(x_n^0, \theta^0)\}_{n=0}^{\infty}$ *is a sequence of compatible periodic hybrid orbits.*
2. *If* $a = 1/2$, b *is a positive odd integer,* $x_0^0 = \frac{r}{2^s}$, *for some* $r, s \in \mathbb{N}$ *with* $s \geq 1$, $1 \leq r < 2^s$ *being odd and* $\theta^0 := \arctan\frac{b\sqrt{3}}{2a+b}$, *then the sequence of compatible closed orbits* $\{\mathscr{O}_n(x_n^0, \theta^0)\}_{n=0}^{\infty}$ *is a sequence of compatible periodic hybrid orbits.*

Proof. Let $r, s \in \mathbb{N}$, with $s \geq 1$ and $1 \leq r < 4^s$, a and b both be positive integers with b being odd and $x_0^0 = \frac{r}{4^s}$. Suppose a line starting at $(x_0^0, 0)$ with slope $\frac{b\sqrt{3}}{2a+b}$ intersects a point in $\mathbb{R}^2$ that would correspond to a lattice point of a lattice comprised of equilateral triangles at scale k. If $m, n, p, q, k \in \mathbb{Z}$, with $k \geq 1$ and $p, q \leq 3^k$, then such a point has the form $(m + p/3^k)u_1 + (n + q/3^k)u_2$. Then, using the equation

for a line in the plane, we find that

$$\left(n + \frac{q}{3^k}\right)\frac{\sqrt{3}}{2} = \frac{b\sqrt{3}}{2a+b}\left(m + \frac{p}{3^k} + \frac{n}{2} + \frac{q}{2\cdot 3^k} - \frac{r}{4^s}\right), \tag{4}$$

$$\left(\frac{3^k n + q}{3^k}\right)\frac{1}{2} = \frac{b}{2a+b}\left(\frac{4^s 3^k m + 4^s p + 2\cdot 4^{s-1}3^k n + 2\cdot 4^{s-1}q - 3^k r}{3^k 4^s}\right), \tag{5}$$

$$2\cdot 4^{s-1}(3^k n + q)(2a+b) = b(4^s 3^k m + 4^s p + 2\cdot 4^{s-1}3^k n + 2\cdot 4^{s-1}q - 3^k r). \tag{6}$$

Since b and r are odd, the left-hand side of Equation (6) is even, but the right-hand side is not. Therefore, our assumption that such a point corresponding to a lattice point at scale k laid on the line beginning at $x_0^0 = r/4^s$ with slope $\frac{b\sqrt{3}}{2a+b}$ was incorrect. It follows that such a line emanating from $x_0^0 = r/4^s$ avoids all points in the boundary of $\Omega(KS_0)$ having finite ternary expansions. By Theorem 26, every orbit in the sequence of compatible orbits must therefore be a periodic hybrid orbit, meaning that $\{\mathcal{O}_n(x_n^0, \theta^0)\}_{n=0}^\infty$ is a sequence of compatible periodic hybrid orbits.

If $a = 1/2$, b is a positive odd integer, $x_0^0 = r/2^s$, with $s \geq 1$ and $1 \leq r < 2^s$, then a similar argument shows that $\{\mathcal{O}_n(x_n^0, \theta^0)\}_{n=0}^\infty$ is a sequence of compatible periodic hybrid orbits. Suppose a line starting at $(x_0^0, 0)$ with slope $\frac{b\sqrt{3}}{2a+b}$ intersects a point in $\mathbb{R}^2$ that would correspond to a lattice point of a lattice comprised of equilateral triangles at scale k. If $m, n, p, q, k \in \mathbb{Z}$, with $k \geq 1$ and $p, q \leq 3^k$, then such a point has the form $(m + p/3^k)u_1 + (n + q/3^k)u_2$. Then, using the equation for a line in the plane, we find that

$$\left(n + \frac{q}{3^k}\right)\frac{\sqrt{3}}{2} = \frac{b\sqrt{3}}{2a+b}\left(m + \frac{p}{3^k} + \frac{n}{2} + \frac{q}{2\cdot 3^k} - \frac{r}{2^s}\right), \tag{7}$$

$$\left(\frac{3^k n + q}{3^k}\right)\frac{1}{2} = \frac{b}{2a+b}\left(\frac{2^s 3^k m + 2^s p + 2^{s-1}3^k n + 2^{s-1}q - 3^k r}{3^k 2^s}\right), \tag{8}$$

$$2^{s-1}(3^k n + q)(2a+b) = b(2^s 3^k m + 2^s p + 2^{s-1}3^k n + 2^{s-1}q - 3^k r). \tag{9}$$

Since b and r are odd and $a = 1/2$, we see that the left-hand side of Equation (9) is even and the right-hand side is not. Therefore, our assumption that such a point corresponding to a lattice point at scale k laid on the line beginning at $x_0^0 = r/2^s$ with slope $\frac{b\sqrt{3}}{2a+b}$ was incorrect. It follows that such a line emanating from $x_0^0 = r/2^s$ avoids all points in the boundary of $\Omega(KS_0)$ having finite ternary expansions. By Theorem 26, every orbit in the sequence of compatible orbits must therefore be a periodic hybrid orbit, meaning that $\{\mathcal{O}_n(x_n^0, \theta^0)\}_{n=0}^\infty$ is a sequence of compatible periodic hybrid orbits. □

Example 28 (A sequence of compatible periodic hybrid orbits)**.** In Figure 12, three periodic hybrid orbits are displayed. These three orbits constitute the first three terms in a sequence of compatible periodic hybrid orbits. If we choose $x_0^0 = \bar{c} \in I$ and θ_0^0 to be an angle such that x_0^0 connects with the midpoint of the lower one-third interval on the side of $\Omega(KS_0)$, we can see that $\mathcal{O}_0(x_0^0, \theta_0^0)$ is a periodic hybrid orbit. More importantly, there are elements of the footprint $\mathcal{F}_0(x_0^0, \theta_0^0)$ with ternary representations of type $[lr, c]$. This observation is key for constructing what we call nontrivial polygonal paths of $\Omega(KS)$, a topic which is discussed in more detail in §5.

Example 29 (A sequence of compatible hook orbits)**.** Let $x_0^0 \in I$ have a ternary representation given by $\overline{rl}$, which is a Cantor point of KS (in the sense of §2.5). Such a point has a value of $3/4$. Considering an orbit of $\Omega(KS_0)$ with an initial direction of $\pi/6$, the ternary representation of the basepoints at which the billiard
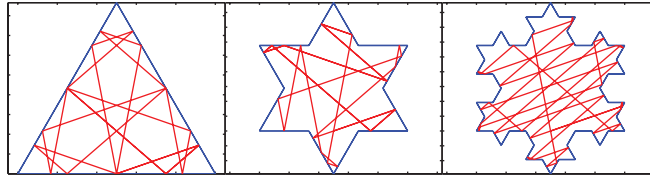
FIGURE 12. Three examples of periodic hybrid orbits. These are the first three elements of the sequence of compatible periodic hybrid orbits described in Example 28.
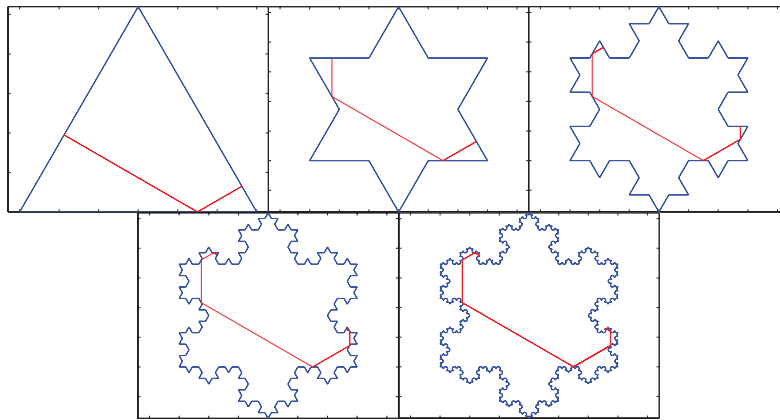

FIGURE 13. An example of a hook orbit. The same initial condition is used in each prefractal billiard.

ball path forms right angles with the sides of $\Omega(KS_0)$ is of the type $[c, lr]$. This is a degenerate periodic hybrid orbit, meaning that it doubles back on itself, and the next orbit in the sequence of compatible periodic hybrid orbits has the initial condition $(x_1^0, \pi/6) = (x_0^0, \pi/6)$. Since the ternary representation of the basepoint of $f_0(x_0^0, \pi/6)$ is $r\bar{c}$ and $\theta_0^0 = \theta_1^0 = \pi/6$, it follows that the basepoint of $f_1(x_1^0, \pi/6)$ is a Cantor point. Then, still in the notation introduced in Remark 2, the basepoint of $f_1^2(x_1^0, \pi/6)$ has a ternary representation of type $[c, lr]$. This same pattern is repeated for every subsequent orbit in the sequence of compatible orbits. As a result, the sequence of compatible orbits forms a sequence of orbits that is converging to a set that is well defined. That is, such a set will be some path with finite length that is effectively determined by the law of reflection in each prefractal approximation.

Such orbits are referred to as *hook orbits* for the fact that they appear to be "hooking" into the Koch snowflake; see Figure 13.

Theorem 30. *If every element $x_0^{k_0} \in \mathcal{F}_0(x_0^0, \theta_0^0)$ has a ternary representation of type $[lr, c]$, then there exists $N \geq 0$ such that $\{\mathcal{O}_n(x_n^0, \theta^0)\}_{n=N}^\infty$ is a constant sequence of compatible periodic hybrid orbits.*

Proof. Recall that the orbit $\mathcal{O}_0(x_0^0, \theta_0^0)$ can be unfolded in the billiard $\Omega(KS_n)$. Each element $x_n^{k_n}$ of the footprint $\mathcal{F}_n(x_n^0, \theta_n^0)$ of the compatible orbit $\mathcal{O}_n(x_n^0, \theta_n^0)$ has a ternary representation of type $[lr, c]$. Since there are finitely many c's in such a representation, there exists N such that the ternary representation of every element
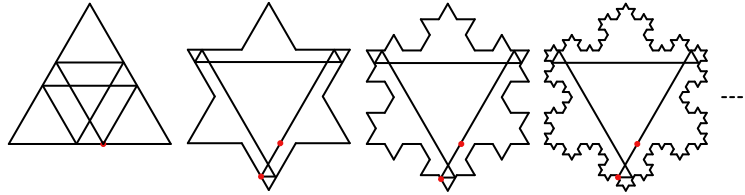
FIGURE 14. An eventually constant sequence of compatible periodic hybrid orbits. We see that the initial basepoint $x_0^0 = 7/12$ lies on the middle third of the unit interval. The basepoint x_1^0 of the compatible initial condition $(x_1^0, \pi/3)$ has a ternary representation of type $[lr, \emptyset]$.

$x_N^{k_N} \in \mathcal{F}_N(x_N^0, \theta_N^0)$ (this being the footprint of a compatible orbit $\mathcal{O}_N(x_N^0, \theta_N^0)$) is of type $[lr, \emptyset]$. As a result, the sequence of compatible periodic hybrid orbits $\{\mathcal{O}_n(x_n^0, \theta^0)\}_{n=N}^{\infty}$ is constant, since every basepoint of every orbit remains fixed for every subsequent prefractal billiard $\Omega(KS_M)$, $M \geq N$. $\qquad\square$

Example 31 (A constant sequence of compatible periodic hybrid orbits). Consider $x_0^0 = 7/12$ in the base of the equilateral triangle. Such a value has a ternary representation of type $[lr, c]$. Consider the initial condition $(x_0^0, \pi/3)$. The sequence of compatible orbits $\{\mathcal{O}_n(x_n^0, \pi/3)\}_{n=1}^{\infty}$ is a constant sequence. This follows from the fact that the ternary representation of x_1^0 is $\overline{rl}$. Moreover, the representation of every basepoint of $\mathcal{O}_n(x_n^0, \pi/3)$ is $\overline{lr}$. In Figure 14, we show the first three orbits in this (eventually) constant sequence of compatible periodic hybrid orbits.

As of now, the only examples of constant sequences of compatible nondegenerate periodic hybrid orbits we can provide are those for which the initial direction is $\pi/3$. Of course, one can construct a constant sequence of compatible periodic hybrid orbits, each with an initial direction of $\pi/6$ or $\pi/2$, but such orbits will be degenerate.

5. **Nontrivial polygonal paths of** $\Omega(KS)$. Consider a periodic hybrid orbit of $\Omega(KS_0)$. Each basepoint $x_0^{k_0}$ of a footprint $\mathcal{F}_0(x_0^0, \theta_0^0)$ has a ternary representation that indicates such a point never corresponds to a ternary point of a side. Hence, the unfolding never hits a corner of any prefractal billiard $\Omega(KS_n)$. As a result, we formulate the following conjecture.

Conjecture 32. *Let* $\mathcal{O}_0(x_0^0, \theta_0^0)$ *be a periodic hybrid orbit of* $\Omega(KS_0)$. *If the basepoints of the footprint* $\mathcal{F}_0(x_0^0, \theta_0^0)$ *are dynamically ordered in such a way that the type of ternary representation alternates between* $[c, lr] \vee [cl, r] \vee [cr, l] \vee [lcr, \emptyset]$ *and* $[lr, \emptyset]$, *then the corresponding sequence of compatible periodic hybrid orbits yields a sequence of basepoints converging to an elusive limit point of the Koch snowflake* KS.

We know that this conjecture is true for some family of sequences of compatible periodic hybrid orbits, as evidenced by the fact that a sequence of compatible hook orbits and the sequence of compatible periodic hybrid orbits given in Figure 12 exhibit such a behavior. In Figure 15, we show exactly the points referred to in Conjecture 32. In this particular case, such points are derived from the sequence of compatible periodic hybrid orbits given in Figure 12.
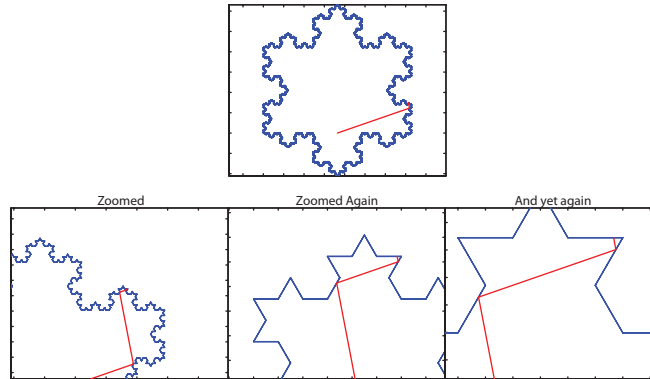
FIGURE 15. A collection of basepoints from successive compatible periodic hybrid orbits converging to an elusive limit point of KS.

As we can see from Figure 15, the sequences of Cantor points determined from a sequence of compatible periodic hybrid orbits can be connected to form what we call a *nontrivial polygonal path of* $\Omega(KS)$. Specifically, for every $n \geq 0$, there exists $N \leq n$ and a sequence of basepoints $\{x_n^{k_n}\}_{n=0}^N$ such that for every $j < N$, $x_j^{k_j}$ has a ternary representation of type $[lr, \emptyset]$ and $x_N^{k_N}$ has a ternary representation of type $[c, lr] \vee [cl, r] \vee [cr, l] \vee [lcr, \emptyset]$. Then each pair $\{x_j^{k_j}, x_{j+1}^{k_{j+1}}\}$, $0 \leq j < N$, can be connected to form a line segment and, collectively, the segments form a path. Then, $\lim_{N \to \infty} x_N^{k_N}$ is an elusive limit point of KS and the collection of segments $\left\{ \overline{x_j^{k_j} x_{j+1}^{k_{j+1}}} \right\}_{j=0}^\infty$ constitutes a nontrivial polygonal path of $\Omega(KS)$. We denote such a path by $\mathscr{N}(x_0^0, \theta_0^0)$.

We next show how to construct two nontrivial polygonal paths that will connect two elusive limit points of the Koch snowflake KS. Consider a sequence of compatible periodic hybrid orbits $\{\mathscr{O}_n(x_n^0, \theta^0)\}_{n=0}^\infty$ that determines a nontrivial polygonal path. Let $\overline{\theta^0} = \theta^0 + \pi$ be the angle made by a vector based at x_0^1 when measured relative to the fixed coordinate system and define $\overline{x_0^0} := x_0^1$. Then the sequence of compatible hybrid periodic orbits $\{\mathscr{O}_n(\overline{x_n^0}, \overline{\theta^0})\}_{n=0}^\infty$ determines a nontrivial polygonal path of KS. Denoting the nontrivial polygonal paths of $\{\mathscr{O}_n(x_n^0, \theta^0)\}_{n=0}^\infty$ and $\{\mathscr{O}_n(\overline{x_n^0}, \overline{\theta^0})\}_{n=0}^\infty$ by $\mathscr{N}(x_0^0, \theta^0)$ and $\mathscr{N}(\overline{x_0^0}, \overline{\theta^0})$, respectively, we see that the concatenation $\mathscr{N}(x_0^0, \theta^0) \cup \mathscr{N}(\overline{x_0^0}, \overline{\theta^0})$ determines a path from one elusive point of KS to another elusive limit point of KS.

As a result, if one is given the fact that an elusive limit point $x^0 \in KS$ is the limit of a sequence of basepoints constituting the vertices of a nontrivial polygonal path, then one can determine a path from x^0 to another elusive limit point $x^1 \in KS$ by following the path determined by the two nontrivial polygonal paths, each being determined by the law of reflection.

6. **Concluding remarks.** We have seen two extremes: sequences of compatible orbits that are (eventually) constant and sequences of compatible orbits with non-trivial limiting behavior. Ultimately, we want to answer the following question: Can one determine the shortest path between two points of the snowflake subject to a well-defined collision in the boundary? Finding an answer to such a question

amounts to determining a suitable law of reflection in the boundary KS. As we have seen in the case of a constant sequence of compatible orbits, for certain initial conditions, it is possible to determine a well-defined orbit of the Koch snowflake. In the case of a sequence of compatible periodic hybrid orbits that determines a nontrivial polygonal path, we have seen a way to connect two elusive limit points via two nontrivial polygonal paths of finite length; cf. §5. We conjecture that such paths constitute subsets of a well-defined orbit of $\Omega(KS)$. That is, once a suitable law of reflection is determined, we expect a nontrivial polygonal path determined from a sequence of compatible periodic hybrid orbits to be a subset of the corresponding orbit.

We note that several of the geometric and topological properties of certain possible periodic orbits (or their footprints) of $\Omega(KS)$ are provided in [13] and [15], along with some experimental evidence in support of a "fractal law of reflection".

Understanding how a billiard ball reflects off of an elusive limit point is at the heart of the 'fractal billiards problem'. In general, fractal snowflakes constitute the canonical examples of fractal billiards. One may perform a similar analysis with similar results for the square snowflake. While not the prototypical examples of a fractal billiard, the T-fractal and a Sierpinski carpet billiard also constitute fractal billiard tables; see Figure 16. Each of these tables contain elusive limit points, and in some ways may be more tractable than a snowflake billiard. Recent work between the second author and Joe P. Chen in [1] extends the results of [2] with the intention of understanding the billiard dynamics on a self-similar Sierpinski carpet billiard table. By further understanding the nature of what are called *nontrivial line segments*, one can determine orbits of a self-similar Sierpinski carpet that never intersect any corners or sides of any deleted squares of any prefractal approximation, save for those of the initial unit square. Of course, the problem is that such orbits do intersect infinitely many elusive limit points of the self-similar Sierpinski carpet, highlighting the core problem of determining dynamics on a fractal billiard table.

Taking a different perspective, the work in progress [14] seeks to understand the nature of the '*fractal flat surface*' by examining the sequence of Veech groups of prefractal flat surfaces. By extending the work of [25], the authors hope to view the prefractal flat surfaces $\mathcal{S}(KS_n)$ as 'rhombic origamis', as opposed to the traditional square tiled surfaces found in [25].

Approaching the problem of determining dynamics on fractal billiard tables from various perspectives may eventually bring about a clearer picture of what should constitute a true fractal billiard. We hope that our work will help lay the foundations for this new subject and spark the interest of other researchers working on related questions and who may provide the additional insights needed for solving these difficult problems.

REFERENCES

[1] J. P. Chen and R. G. Niemeyer, *Periodic billiard orbits of self-similar Sierpinski carpets*, in Preparation, (2012).

[2] E. Durane-Cartagena and J. T. Tyson, *Rectifiable curves in Sierpiński carpets*, to appear in Indiana Univ. Math. J., (2011).

[3] K. J. Falconer, "Fractal Geometry: Mathematical Foundations and Applications," John Wiley & Sons, Chichester, 1990. (2nd edition, 2003.)
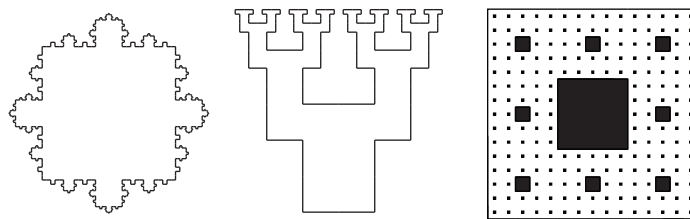
FIGURE 16. The square snowflake, T-fractal and a Sierpinski carpet.

[4] G. Galperin, Ya. B. Vorobets and A. M. Stepin, *Periodic billiard trajectories in polygons*, Russian Math. Surveys, **47** (1992), 5–80.

[5] E. Gutkin, *Billiards in polygons: Survey of recent results*, J. Stat. Phys., **83** (1996), 7–26.

[6] E. Gutkin, *Billiards on almost integrable polyhedral surfaces*, Erg. Th. and Dyn. Syst., **4** (1984), 569–584.

[7] E. Gutkin and C. Judge, *The geometry and arithmetic of translation surfaces with applications to polygonal billiards*, Math. Res. Lett., **3** (1996), 391–403.

[8] E. Gutkin and C. Judge, *Affine mappings of translation surfaces: Geometry and arithmetic*, Duke Math. J., **103** (2000), 191–213.

[9] P. Hubert and T. Schmidt, *An introduction to Veech surfaces*, in "Handbook of Dynamical Systems" **1B** (eds. A. Katok and B. Hasselblatt), Elsevier, Amsterdam, (2006), 501–526.

[10] A. Katok and B. Hasselblatt, "A First Course in Dynamics: With a Panorama of Recent Developments," Cambridge Univ. Press, Cambridge, 2003.

[11] A. Katok and A. Zemlyakov, *Topological transitivity of billiards in polygons*, Math. Notes, **18** (1975), 760–764.

[12] M. L. Lapidus and R. G. Niemeyer, *Towards the Koch snowflake fractal billiard—Computer experiments and mathematical conjectures*, in "Gems in Experimental Mathematics" (eds. T. Amdeberhan, L. A. Medina and V. H. Moll), Contemporary Mathematics, Amer. Math. Soc., Providence, RI, **517** (2010), 231–263. [E-print: arXiv:math.DS.0912.3948v1, 2009.]

[13] M. L. Lapidus and R. G. Niemeyer, *Families of periodic orbits of the Koch snowflake fractal billiard*, 63 pages, e-print, `arXiv:1105.0737v1`, (2011).

[14] M. L. Lapidus and R. G. Niemeyer, *Veech groups Γ_n of the Koch snowflake prefractal flat surfaces $\mathcal{S}(KS_n)$*, in Progress, 2012.

[15] M. L. Lapidus and R. G. Niemeyer, *Experimental evidence in support of a fractal law of reflection*, in progress, (2012).

[16] W. S. Massey, "Algebraic Topology: An Introduction," Springer-Verlag, New York, 1977.

[17] H. Masur, *Closed trajectories for quadratic differentials with an applications to billiards*, Duke Math. J., **53** (1986), 307–314.

[18] H. Masur and S. Tabachnikov, *Rational billiards and flat structures*, in "Handbook of Dynamical Systems" **1A** (eds. A. Katok and B. Hasselblatt), Elsevier, Amsterdam, (2002), 1015–1090.

[19] J. Smillie, *Dynamics of billiard flow in rational polygons*, in "Dynamical Systems" Encyclopedia of Math. Sciences, **100**, Math. Physics 1 (ed. Ya. G. Sinai), Springer-Verlag, New York, (2000), 360–382.

[20] S. Tabachnikov, "Billiards," Panoramas et Synthèses, Soc. Math. France, Paris, 1995.

[21] S. Tabachnikov, "Geometry and Billiards," Amer. Math. Soc., Providence, RI, 2005.

[22] W. A. Veech, *The billiard in a regular polygon*, Geom. Funct. Anal., **2** (1992), 341–379.

[23] W. A. Veech, *Flat surfaces*, Amer. J. Math., **115** (1993), 589–689.

[24] Ya. B. Vorobets, *Plane structures and billiards in rational polygons: The Veech alternative*, Russian Math. Surveys, **51** (1996), 779–817.

[25] G. Weitze-Schmithüsen, *An algorithm for finding the Veech group of an origami*, Experimental Mathematics, **13** (2004), 459–472.

[26] A. Zorich, *Flat surfaces*, in "Frontiers in Number Theory, Physics and Geometry" **I** (eds. P. Cartier, et al.,), Springer-Verlag, Berlin, (2002), 439–585.

E-mail address: lapidus@math.ucr.edu;niemeyer@math.ucr.edu